Environment International 125 (2019) 386–398

Contents lists available at ScienceDirect

Environment International

journal homepage: www.elsevier.com/locate/envint

Comprehensively assessing the drivers of future air quality in California

Shupeng Zhu[a], Jeremy R. Horne[a], Michael Mac Kinnon[b], G.S. Samuelsen[b], Donald Dabdub[a,*]

[a] Computational Environmental Sciences Laboratory, University of California, Irvine, CA 92697, USA
[b] Advanced Power and Energy Program, University of California, Irvine, CA 92697, USA

ARTICLE INFO

Handling Editor: Xavier Querol

ABSTRACT

In this study we analyze the impact of major drivers of future air quality, both separately and simultaneously, for the year 2035 in three major California air basins: the South Coast Air Basin (SoCAB), the San Francisco Bay Area (SFBA), and the San Joaquin Valley (SJV). A variety of scenarios are considered based on changes in climate-driven meteorological conditions and both biogenic and anthropogenic emissions. Anthropogenic emissions are based on (1) the California Air Resources Board (CARB) California Emissions Projection Analysis Model (CEPAM), (2) increases in electric sector emissions due to climate change, and (3) aggressive adoption of alternative energy technologies electrification of end-use technologies, and energy efficiency measures.

Results indicate that climate-driven changes in meteorological conditions will significantly alter day-to-day variations in future ozone and $PM_{2.5}$ concentrations, likely increasing the frequency and severity of pollution periods in regions that already experience poor air quality and increasing health risks from pollutant exposure. Increases in biogenic and anthropogenic emissions due to climate change are important during the summer seasons, but have little effect on pollutant concentrations during the winter. Results also indicate that controlling anthropogenic emissions will play a critical role in mitigating climate-driven increases in both ozone and $PM_{2.5}$ concentrations in the most populated areas of California. In the absence of anthropogenic emissions controls, climate change will worsen ozone air quality throughout the state, increasing exceedances of ambient air quality standards. If planned reductions in anthropogenic emissions are implemented, ozone air quality throughout the less urban areas of the state may be improved in the year 2035, but regions such as the SoCAB and the east SFBA will likely continue to experience high ozone concentrations throughout the summer season. Climate change and anthropogenic emissions controls are both found to decrease wintertime $PM_{2.5}$ concentrations in the SJV, eliminating nearly all exceedances of $PM_{2.5}$ National Ambient Air Quality Standards (NAAQS) in the year 2035. However, reductions in anthropogenic emissions are unable to fully mitigate the impact of climate change on $PM_{2.5}$ concentrations in the SoCAB and east SFBA. Thus, while future air quality in the SJV is projected to be improved in the year 2035, air quality in the SoCAB and east SFBA will remain similar or marginally worsen compared to present day levels. Conversely, we find that aggressive adoption of alternative energy technologies including renewable resources, electrification of end-use technologies, and energy efficiency measures can offset the impacts of climate change. Overall, the two main drivers for air quality in 2035 are changes in meteorological conditions due to climate change and reductions in anthropogenic emissions.

1. Introduction

Future air quality, especially aerosols and ozone, will be governed by a range of factors including the physical impacts of climate change and socioeconomic factors such as emission control efforts, demands in energy end-use sectors, and the deployment of alternative transportation and electricity generation technologies (Loughlin et al., 2011; Collet et al., 2014; Nsanzineza et al., 2017; Zhang et al., 2017; Zapata et al., 2018). While the impact of some of these factors on air quality has been studied from an individual perspective (Racherla and Adams, 2006; Mahmud et al., 2010; Mahmud et al., 2012; Ebrahimi et al., 2018; Kinnon et al., 2019), there is a lack of information considering them from a *holistic* perspective: e.g., analysis of the combined impacts, comparison among factors using a consistent modeling platform, and analysis of the relative importance of controlling air pollutant precursor emissions to the potential physical impacts of climate change. Although some studies have examined the impact of climate change on regional air quality in California, most focus exclusively on the southern California South Coast Air Basin (SoCAB), a domain centered over Los Angeles. The impact of future changes in climate and emissions on air

* Corresponding author.
E-mail address: ddabdub@uci.edu (D. Dabdub).

https://doi.org/10.1016/j.envint.2019.02.007
Received 7 September 2018; Received in revised form 7 January 2019; Accepted 2 February 2019
Available online 08 February 2019

quality in the San Francisco Bay Area (SFBA) and the San Joaquin Valley (SJV) of California, which are designated non-attainment area for both ozone and $PM_{2.5}$ ambient air quality standards (CARB, 2017a; U.S. EPA, 2018), warrants further study. As of April 2018, there are > 35 counties in California designated as nonattainment areas for criteria pollutants such as ozone, PM10, and $PM_{2.5}$ (U.S. EPA, 2018). Therefore, there is a need for a comprehensive assessment of future air quality in California at the state level using a high-resolution air quality model that can resolve local changes in air quality due to the major drivers of pollutant concentrations.

Air pollution and climate change are inextricably linked. Not only are greenhouses gases (GHG) and air pollutants generally emitted from the same sources, but many air pollutants can cause changes in climate due to their interactions with solar radiation (Fiore et al., 2012; Fiore et al., 2015; Fuzzi et al., 2015; Von Schneidemesser et al., 2015; Lee et al., 2016; Erickson and Jennings, 2017). Climate-driven changes in meteorology impact both direct emissions and the formation of secondary pollutants through changes in temperature and atmospheric water vapor content, among other meteorological variables (Jacob and Winner, 2009; Fiore et al., 2012; Fiore et al., 2015; Von Schneidemesser et al., 2015; Kinney, 2018). The transport, concentration, and lifetime of atmospheric constituents is also impacted by changes in meteorological conditions such as mixing height, circulation patterns, and precipitation(Jacob and Winner, 2009; Fiore et al., 2012; Fiore et al., 2015; Von Schneidemesser et al., 2015; Kinney, 2018). Climate change is projected to cause increases in the severity and frequency of pollution periods in the future due to a weaker global circulation and more stagnant conditions (Jacob and Winner, 2009; Fiore et al., 2015; Von Schneidemesser et al., 2015). Countless studies have examined the links between air quality and climate change to better understand the highly coupled nature of these two environmental issues. Recent modeling studies and comprehensive reviews on these topics advance our understanding and stress the importance of utilizing an integrated approach to simultaneously reduce air pollution and mitigate climate change (Fiore et al., 2012; Fiore et al., 2015; Fuzzi et al., 2015; Von Schneidemesser et al., 2015; Lee et al., 2016; Erickson and Jennings, 2017).

The impact of climate change on air quality has been studied at the global scale (Brasseur et al., 2006; Liao et al., 2006; Racherla and Adams, 2006; Heald et al., 2008; Lin et al., 2016), the national scale (Kelly et al., 2012; Gao et al., 2013; Fann et al., 2015; Val Martin et al., 2015; He et al., 2016; Lee et al., 2016; Campbell et al., 2018), and the regional scale in California (Aw and Kleeman, 2003; Carreras-Sospedra et al., 2006; Steiner et al., 2006; Kleeman, 2008; Mahmud et al., 2008, 2010; Millstein and Harley, 2009; Mahmud et al., 2012). Some modeling studies examined the impact of changes in individual meteorological parameters on air quality in southern California (Aw and Kleeman, 2003; Steiner et al., 2006; Millstein and Harley, 2009; Horne and Dabdub, 2017). These studies found that among the different meteorological parameters perturbed, temperature increases typically played the most important role in determining the overall impact of climate change on both gas- and particle-phase pollutants. Increasing temperatures generally causes increases in ozone concentrations in polluted regions due to accelerated reaction rates but can have the opposite effect on aerosols due to decreased gas to particle partitioning. However, the overall effect of climate change on aerosol concentrations remains uncertain, with large variability in projections between different studies and models, and within individual studies depending on geographic location (Racherla and Adams, 2006; Jacob and Winner, 2009; Fiore et al., 2012; Fuzzi et al., 2015). Climate change has also been shown to impact emissions from energy systems, including increases in vehicle emissions correlating with surface temperatures (Motallebi et al., 2008). Overall, most studies concluded that additional emissions controls will need to be implemented to reduce air pollutant concentrations under the less favorable meteorological conditions induced by climate change (Jacob and Winner, 2009; Fiore et al., 2012; Fiore et al., 2015; Von Schneidemesser et al., 2015). Additionally, the regional air quality impacts of alternative energy technologies has been considered within the context of achieving GHG reductions, including the deployment of renewable resources and alternative transportation technologies (Jacobson et al., 2005; Hart and Jacobson, 2012; Jacobson et al., 2015; Morrison et al., 2015). These studies demonstrate the significant potential benefits to human health and advanced energy technologies can be achieved in future energy systems. Although existing modeling studies have furthered our understanding of the individual and combined effects of meteorological variations on individual pollutant concentrations, they did not provide a comprehensive assessment of future air quality in California. Furthermore, many studies concluded that the impact of future emissions changes on air quality is more uncertain than the impacts of climate change and stressed the need for examining the impact of climate change on air quality concurrently with the effect of potential future changes in biogenic and anthropogenic emissions (Jacob and Winner, 2009; Fiore et al., 2012; Fiore et al., 2015; Von Schneidemesser et al., 2015).

In this study we consider a range of scenarios to quantify and compare the potential air quality impacts of future changes in climate and emissions and provide a comprehensive assessment of future air quality in California. We assess the effectiveness of emissions control strategies and determine if the expected reductions in air pollutant and precursor emissions will be sufficient to achieve air quality targets in a changing climate. We focus on California because it contains a wide range of climatic and geographic conditions and consistently experiences some of the worst air quality in the nation in highly populated areas (CARB, 2017a; U.S. EPA, 2018), posing serious risks to human health (Ebi and McGregor, 2008; Kampa and Castanas, 2008; Tai et al., 2010). We conduct simulations spanning several months and for both summer and winter periods to provide a complete assessment of future air quality and capture seasonal variations in climate change impacts and pollutant concentrations. The year 2035 is selected to reduce the uncertainty associated with long-term projections of both climate and emissions in an evolving regulatory environment. The CMAQ model is run with a high spatial resolution using the SAPRC-07 chemical mechanism to provide state-of-the-science model predictions, and results are compared to ambient measurements to evaluate model performance. This work also quantifies the impact of climate-correlated changes in building energy consumption and considers the potential impact of energy efficiency strategies and wide-spread adoption of renewable electricity in tandem with the electrification of end-use energy sectors. The associated socioeconomic impacts are also estimated based on health impact assessment via the Environmental Benefits Mapping and Analysis Program-Community Edition (BenMAP-CE, available at http://www.epa.gov/airquality/benmap/ce.html). The results of this study are not intended to be definitive forecasts of future air quality, but rather provide insight as to the importance and impact of different drivers of air quality while providing an updated picture of potential air pollutant concentrations in the future.

We begin the next section with a summary of the methods used in our analysis and a description of the scenarios we consider. The following subsections describe the CMAQ model formulation and the generation of the inputs required to conduct the air quality simulations. Results and discussion are presented in Section 3, followed by conclusions in Section 4.

2. Model and methodology

In this study, air quality in California is simulated using the Community Multiscale Air Quality Modeling System (CMAQ, v5.2). Seven air quality scenarios (including the baseline) are designed to investigate the individual and combined effect of different air quality drivers as summarized in Table 1. Details about the modeling tools and the air quality drivers used in different scenarios will be presented in

Table 1
Name and description of each scenario considered in this study including the meteorology, biogenic emissions, and anthropogenic emissions used in the model simulations.

Scenario	Meteorology	Biogenic emissions	Anthropogenic emissions	Description
BASE	2012	2012	2012	Reference case to determine changes in emissions and air quality
CARB	2012	2012	2035 with CARB controls	Assess effectiveness of CARB emission control strategies (without climate change)
TECH	2012	2012	2035 with CARB controls and new technology	Assess air quality benefits of expanded emission reduction strategies, including efficiency measures, renewable power and end-use electrification
MET	2035 based on RCP 4.5	2012	2012	Isolate the impact of climate-driven changes in meteorological conditions on air quality with no emissions changes
CLIM	2035 based on RCP 4.5	2035 using RCP4.5 in MEGAN	2035 with RCP4.5 building load	Assess the overall impact of near-term climate change on air quality without anthropogenic emissions controls
FUTR-CARB	2035 based on RCP 4.5	2035 using RCP4.5 in MEGAN	2035 with CARB + RCP4.5 building load	Assess effectiveness of CARB emission control strategies (with climate change)
FUTR+	2035 based on RCP 4.5	2035 using RCP4.5 in MEGAN	2035 with CARB+TECH and RCP4.5 building load	Comprehensively assess future air quality in California with climate-driven changes in meteorology and emissions and CARB/TECH emissions controls implemented

this section.

2.1. CMAQ model formulation

Air quality simulations are performed using the Community Multiscale Air Quality Modeling System (CMAQ, v5.2) with the SAPRC-07 chemical mechanism (Carter, 2010) for gas phase chemistry and the AERO6 module (Pye et al., 2013) for aerosol dynamics. The model domain is the same as Benosa et al. (2018), which covers the entire state of California and part of Nevada with a 4 km × 4 km horizontal resolution as shown in (Fig. S2). The focus of this study is the changes in near-surface air quality in the state of California. The boundary conditions are generated from the Model for Ozone and Related Chemical Tracers (Mozart v4.0) (Emmons et al., 2010). The static initial condition from default CMAQ settings are used, and the first 10 days of each period are considered as model spin up and therefore are not included in the analysis of the results. The model performance in the base case simulations is evaluated by comparison with observation data from U.S. Environmental Protection Agency's (U.S. EPA) Air Quality System (AQS) for hourly O_3 and $PM_{2.5}$. Definitions of the statistical parameters used to evaluate model performance are shown in Table S4. Both ozone and PM performance satisfies the recommended performance criteria proposed by (Emery et al., 2017), with normalized mean bias (NMB) < ± 15%, normalized mean error (NME) < 25% and correlation > 50% for O_3, and NMB < ± 30%, NME < 50% and correlation > 40% for $PM_{2.5}$ (Table 2). The averaged time series between model simulation results and observation data for all observation sites are presented in Fig. S3. The model exhibits good correlation with observational data, with the best model performance for O_3 in the summer and $PM_{2.5}$ in the winter. In this study, the air quality analyses are focused on summer O_3 and winter $PM_{2.5}$, as they have exhibited the best model performance and are the dominant air pollutants in these periods.

2.2. Meteorology

Meteorological inputs for CMAQ are generated for a two-month winter period spanning from January 1 to February 28 and a two-month summer period spanning from July 1 to August 31 (months modeled correspond to base year 2012). Those four months are selected to cover some of the coldest (January & February) and hottest (July & August) periods of a year in California (see Fig. S4). Those four months are also representative of seasonal residential energy usage based on data from three major electricity providers in California (See Fig. S5). Meteorological conditions are generated using the Advanced Research Weather Research and Forecasting Model (WRF-ARW, version 3.7), with the MODIS land use database (Friedl et al., 2010) and the YSU parameterization (Hong et al., 2006) for the planetary boundary layer.

Baseline meteorological conditions for the year 2012 are based on (Final) Operational Global Analysis data (NCEP, 2000). The year 2012 is selected because the most recent and detailed emission inventory available for California is based on data generated for the year 2012. Moreover, the average temperature in 2012 is nearly identical to the

Table 2
Comparison of hourly averaged O_3 (ppb) and $PM_{2.5}$ (μg/m^3) between simulation results and observations from the AQS network for the winter period and the summer period, respectively. A 20 ppb cutoff is used to filter values. (Obs. stands for observation; Sim. stands for simulation.)

	Obs. mean	Sim. mean	Correlation (%)	NMB (%)	NME (%)
O_3 Winter	22.99	25.48	79.1	10.8	22.8
O_3 summer	37.98	41.11	92.2	8.2	11.3
$PM_{2.5}$ Winter	10.77	11.09	77.4	3.0	22.8
$PM_{2.5}$ Summer	8.67	10.08	65.7	16.4	26.2

average temperature in last ten years based on measurements from the National Oceanic and Atmospheric Administration (NOAA) (See fig. S4), making it representative of present-day climate. These baseline meteorological conditions are used to simulate both summer and winter periods in the BASE, CARB, and TECH scenarios.

Meteorology for the climate impact studies are based on the global bias-corrected climate model output data for the year 2035 from the Community Earth System Model (CESM1) that participated in phase 5 of the Coupled Model Intercomparison Experiment (CMIP5) (Giorgetta et al., 2013). These simulations supported the Intergovernmental Panel on Climate Change Fifth Assessment Report (IPCC., 2014). Meteorology is interpreted for the winter period (Jan. & Feb.) and the summer period (Jul. & Aug.) based on Representative Concentration Pathway (RCP) future scenario (RCP4.5) datasets (Monaghan et al., 2014). The year 2035 is chosen to reflect a near future scenario and it is also the furthest future year available in the anthropogenic emission control model used in this study (see Section 2.3). These climate-impacted meteorological conditions are used for the MET, CLIM, FUTR-CARB, and FUTR+ scenarios.

2.3. Anthropogenic emissions

Baseline anthropogenic emissions for the year 2012 are calculated using the Sparse Matrix Operator Kernel Emissions (SMOKE) modeling system. The 2012 emissions inventory used in this study is based on the California Air Resources Board (CARB) 2012 inventory (CARB, 2013). It is generated based on emission data from area sources, point sources, and mobile sources. The 2012 anthropogenic emissions are used in the BASE and MET scenarios.

The SMOKE modeling system is also used to generate anthropogenic emissions for the year 2035 based on three main assumptions:

1. The growth and control in anthropogenic emissions projected by CARB in the CEPAM 2016 SIP – Standard Emission Tool (CARB, 2016).
2. Increases in electric sector emissions that occur in response to increased building energy consumption due to climate change (Franco and Sanstad, 2008).
3. Assumed rapid adoption of renewable electricity generation in tandem with efficiency measures and end-use electrification technologies in pursuit of significant greenhouse gas emission reductions (Mahone et al., 2018).

The 2035 anthropogenic emissions used in the CARB, TECH, FUTR-CARB and FUTR+ scenarios include expected emission control strategies developed by CARB to improve air quality and reduce human exposure to air pollutants. These emissions control strategies are based on the CEPAM: 2016 SIP – Standard Emission Tool (CARB, 2017b) and include current policy and regulatory measures, e.g., policy mandated increases in renewable resources and control measures to reduce emissions from on-road transportation sources. CEPAM provides grown and controlled emissions by source category for all criteria pollutant species required for AQ modeling including NO_X, NH_3, PM, CO, TOG, and SO_x. From CEPAM, emissions for stationary sources can be estimated for future years, including those from fuel combustion for electricity generation, commercial and residential buildings, manufacturing, petroleum refining, and other industrial sources. Additionally, emissions from mobile sources including light-, medium- and heavy-duty vehicles (LDV, MDV, HDV), and non-road sources (e.g., agricultural and construction vehicles, ships, and aircraft) are resolved. CEPAM projections account for the various factors influencing energy system emissions including growth in demands and control strategies developed in California to support the National Ambient Air Quality Standards (NAAQS) attainment requirements. For example, though NO_X emission increase by 10% in 2035 for stationary sources due to growing population and energy demand, emissions from LDV decreased by 84% due to the assumed deployment of more efficient vehicles and the deployment of zero emission vehicle technologies. Detailed emission changes for criteria pollutant species can be found in Table S2.

In the CLIM and FUTR+ scenarios, 2035 anthropogenic emissions are affected by changes in electric sector emissions that occur in response to changes in building energy consumption. For example, higher summer temperature due to climate change (RCP4.5) will increase the demand for indoor air conditioning and leads to higher building energy consumption. Thus, the increases in electric sector emissions due to climate change are calculated based on the building electricity demand curve developed by (Franco and Sanstad, 2008), which can be described by the following equation:

$$y = 1.0851x^3 + 1118.9x^2 - 27629x + 789045 \quad (1)$$

Where x represents the average daily temperature (°C), and y is the daily electricity demand (MWh). The electricity demand is calculated separately for each model grid cell and for each simulation day using Eq. (1) with the different meteorological conditions (2012 baseline and 2035 RCP4.5) and weighted by population distributions to filter cells with no residents. By assuming a linear response between the emission of electricity generation sector and electricity demand, the scaling factors for electric sector emissions are calculated by using the ratio between the total population weighted electricity demand under the 2035 RCP4.5 scenario and the 2012 baseline. For scenarios using 2035 RCP4.5 meteorology, the total electricity demand decreased by 1.5% in winter due a reduction in heating demand under warmer conditions, while the demand increased by 7.8% in the summer due to the increased usage of heating, ventilation, and air conditioning (HVAC) systems.

In the TECH and FUTR+ scenarios, we consider how rapid adoption renewable electricity generation in tandem with efficiency measures in all energy end-use sectors (i.e., transportation, industry, residential and commercial buildings) and end-use electrification technologies in pursuit of significant greenhouse gas emission reductions can potentially impact emissions and air quality. In brief, results from a techno-economic model called the California PATHWAYS model are used to consider the potential emissions impacts of widespread adoption of renewable electricity in tandem with energy efficiency and conservation measures, and electrification of transportation applications. PATHWAYS is a "bottom-up" scenario model with detailed technology representation of the commercial and residential building, industrial, transportation, and electricity sectors and explicitly models stocks and replacement of various end-uses (Williams et al., 2012). PATHWAYS is used to evaluate long-term energy scenarios through 2050 to determine options and costs for California to achieve mandated greenhouse gas emission reduction goals (Table S3). Model output for the High Electrification case provided in (Mahone et al., 2018) is used to grow the base year inventory to the year 2035 accounting for mitigation measures implemented in all sectors. An overview of the assumed measures can be found in the Supporting Information (SI) in Table S1. Increases in energy efficiency and the electrification of appliances yield emission reductions from residential and commercial buildings. Significant increases in alternative fueled vehicles are assumed in light-, medium-, and heavy-duty vehicles including battery electric, plug-in hybrid electric, hybrid electric, fuel cell electric, and compressed natural gas technologies (See Fig. S1). Growth in electrification also occurs in rail and port technologies, and harbor craft. Efficiency measures provide emission reductions from the industrial sector, including petroleum refineries and oil and gas extraction activities. Increased efficiency measures and the integration of renewable energy also reduce emissions from the electricity generation sector. For a complete description of the methodology used to project future changes in emissions in this scenario the reader is referred to (Mahone et al., 2018).

Table S3 compares the emission changes in both the CARB and TECH scenarios with the baseline, which shows a more aggressive emission reduction in the TECH scenario compared to the CARB scenario. Direct PM is the only pollutant that is projected to have small emission increases in both scenarios, largely due to population and economic growth. However, as most of $PM_{2.5}$ pollution is caused by secondary PM, such small increase of direct PM emissions is unlikely to impact total $PM_{2.5}$ mitigation (CARB, 2005).

The FUTR+ scenario uses 2035 anthropogenic emissions with consideration of all three factors described above, combining CARB emissions projections with new technology adoption and climate-driven changes in building energy consumption. Changes in emissions of NO_X, VOC, NH_3, and total PM for the FUTR+ scenario versus the BASE scenario are shown in Fig. S7 and Fig. S8 for the summer and winter periods, respectively.

2.4. Biogenic emissions

Biogenic emissions in all scenarios are calculated using the Model of Emissions of Gases and Aerosols from Nature (MEGAN) version 2.1 (Guenther et al., 2006). The MEGAN model requires as input meteorological conditions to determine the magnitude and spatial and temporal distribution of biogenic emissions. Thus, biogenic emissions for the year 2012 that are used in the BASE, CARB, MET, and TECH scenarios are calculated using baseline meteorological conditions for that year. Biogenic emissions in the CLIM FURT-CARB, and FUTR+ scenarios are calculated using the climate-impacted meteorology for the year 2035 based on RCP4.5. Fig. S9 shows the difference in biogenic VOC emissions when using 2035 RCP4.5 meteorology compared with 2012 baseline meteorology. In the summer period, total biogenic emissions increase by 33%, due almost entirely to increases in biogenic VOC emissions (32%). The largest increases occur in the SoCAB and the Sierra Nevada Mountains, with smaller increases occurring near the coast across most of the state. During the winter period, there are only small changes in biogenic emissions due to climate change. On average, wintertime biogenic emissions increase by < 1%, with increases in some areas and decreases in others. Many of the areas along the coast that experience increases during the summer period show decreases during the winter period. Fig. S10 summarized the total emission changes in different control scenarios compares to BASE scenario for both winter and summer period. The climate impact is most reflected in VOC emissions changes and has a much more significant impact during summer period.

2.5. Air quality assessment

Changes in air quality are quantified by using several different metrics, examining both spatially averaged and temporally averaged changes in air pollutant concentrations. To be consistent with ambient air quality standards, we compute maximum daily 8-h average (MD8h) concentrations for ozone and 24-h average concentrations for $PM_{2.5}$. The spatial dependence of changes in air quality is shown in two ways. First, the maximum MD8h ozone that occurs in each model grid cell is calculated for the summer period (Fig. 1), and the maximum 24-h average $PM_{2.5}$ concentration that occurs in each model grid cell extracted for the winter period (Fig. 2). Second, for each grid cell in each scenario, the number of days the (1) 70 ppb MD8h ozone air quality standard is exceeded during the summer period (Fig. 4) and (2) the number of days the 35 μg/m^3 24-h average $PM_{2.5}$ NAAQS is exceeded during the winter period (Fig. 6) is determined. To capture the temporal dependence of changes in ozone and $PM_{2.5}$ concentrations, spatially-averaged concentrations of these pollutants in two subdomains of particular interest in California are computed: (1) the SoCAB and (2) the SJV. The SoCAB is centered over the Los Angeles megacity and contains highly populated regions including parts of Los Angeles, Orange, San Bernardino, and Riverside Counties. The SoCAB is well known for its frequent ozone pollution periods during the summer period and severe health risk due to its population density. The SJV region is home to large-scale agricultural operations and contains most of the San Joaquin Valley Air Pollution Control District, as well as parts of Mariposa, San Luis Obispo, and Monterey Bay counties. The SJV is constantly plagued by $PM_{2.5}$ pollution due to its topographic and climate condition, especially during the winter season. The location and spatial extent of these two regions used in the calculations is shown in Fig. S2. Each region contains a unique blend of different emissions sources, meteorological conditions, and geography. Additionally, these two regions include numerous counties that are designated nonattainment areas for both ozone and $PM_{2.5}$ ambient air quality standards and typically experience some of the worst air quality in the nation (EPA, 2018). Both averaged hourly diurnal ozone concentration and day-to-day variations in MD8h ozone for SoCAB and SJV are calculated along with corresponding temperature variations for different climate assumptions (Fig. 3). The same type of plot is also made for averaged hourly diurnal $PM_{2.5}$ concentration and daily variations of 24-h average $PM_{2.5}$ concentrations, as shown in Fig. 5. A third subdomain, the SFBA, is also marked on Fig. S2. Although it is not used in the temporal analysis due to its similar urban characteristic as SoCAB, it is one of the most populated area in California and found to be one of the most impacted regions in the climate change scenarios.

2.6. Health impact assessment

Following Shen et al. (2017) the environmental Benefits Mapping and Analysis Program—Community Edition (BenMAP-CE) version 1.3 (Davidson et al., 2007; Sacks et al., 2018) is used to quantify and assess the health impacts of ozone and $PM_{2.5}$ concentration changes. California population statistics for 2012 from Land scan data (ORNL, 2016) are grown to 2035 using projections from the California Department of Finance (California DOF, 2017). Baseline incidence rates for mortality and morbidity at the county level by five-year age groups are from the results of a review of the literature (Industrial Economics, 2016c). Similarly, concentration-response (C-R) functions and valuation functions for mortality and morbidity are selected from a thorough literature review (Industrial Economics, 2016b, 2016a) (Industrial Economics and Lisa Robinson, 2016b, 2016a). Short-term health effects are reported for the CARB, TECH, CLIM, FUTR-CARB and FUTR+ scenario as shown on Fig. 7.

3. Future air quality

In the BASE scenario, high MD8h ozone concentration (> 100 ppb) can be found in SoCAB, SFBA and SJV during the summer period, with peak concentration of 179 ppb occurring in the SoCAB (See Fig. 1). Fig. 4 shows large areas of southern California and parts of the SJV exceed the 8-h ozone standards for more than half of the summer period (26 days or more out of 51 days), while SFBA has much fewer exceedances. A good correlation is found between day-to-day variations in MD8h ozone concentrations and daily averaged temperatures, as shown in Fig. 3. Peak ozone concentrations typically occur around 3:00 PM local time according to the diurnal profile in Fig. 3.

During the winter period, high (> 67 μg/m^3) 24-h average $PM_{2.5}$ concentrations can be found mainly in SJV, the urban center in SoCAB and inland area of SFBA (see Fig. 2). These same areas frequently exceed the 24-h average $PM_{2.5}$ NAAQS of 35 μg/m^3 throughout the winter period, with the greatest number of exceedances occurring in the SJV (Fig. 6). $PM_{2.5}$ concentrations in both the SoCAB and the SJV show significant day-to-day variability (see Fig. 5). Unlike ozone, daily variations in $PM_{2.5}$ concentrations are generally not directly correlated with daily average temperatures. As noted in previous studies, other meteorological variables such as humidity, mixing height, circulation patterns, and precipitation strongly influence the formation, transport, and removal of particulate matter in the atmosphere (Jacob and Winner, 2009; Fiore et al., 2012; Fiore et al., 2015; Von Schneidemesser et al., 2015; Kinney, 2018). The diurnal profile shows a peak concentration for morning rush hours in SoCAB, while in SJV constant high

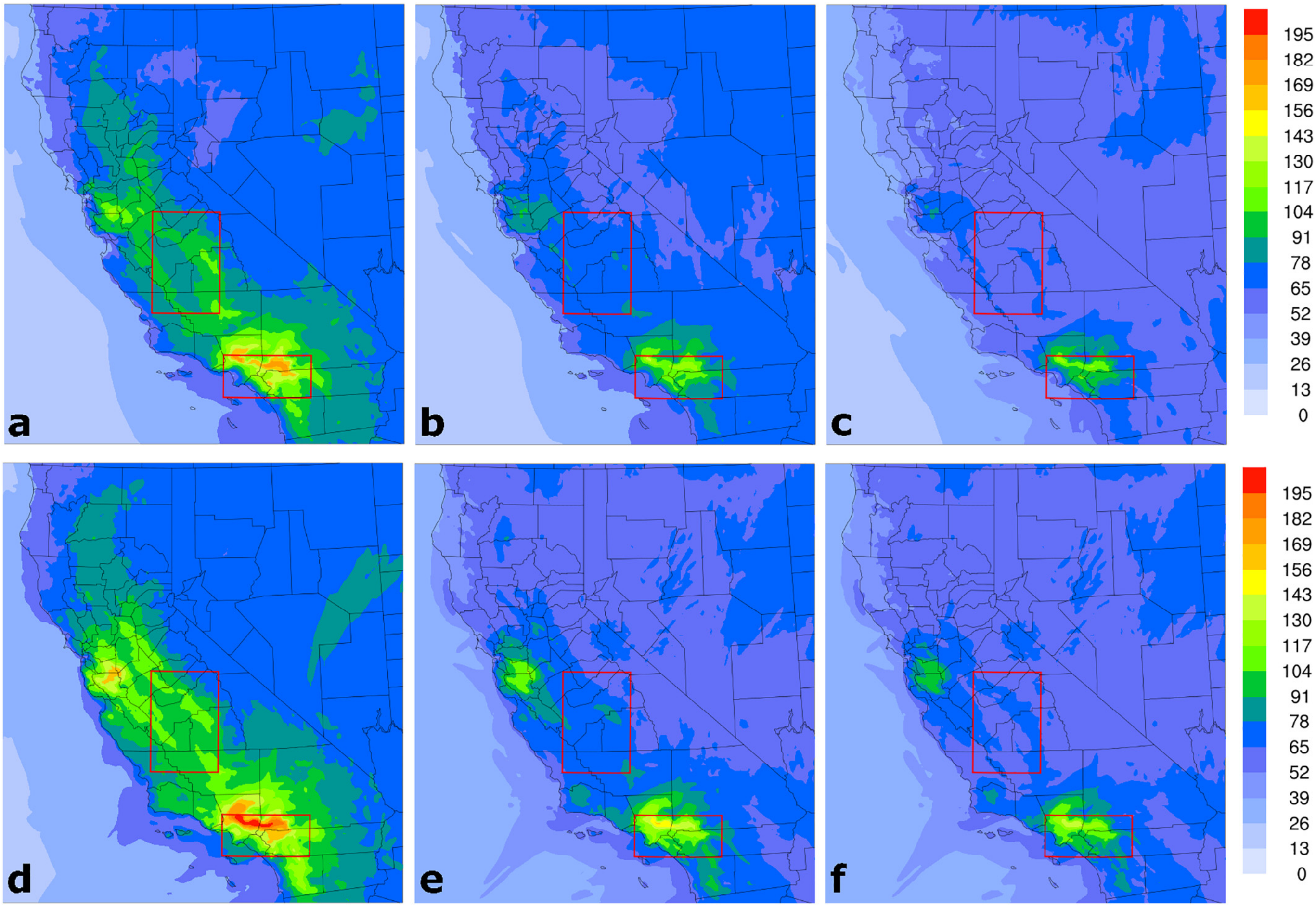

Fig. 1. Peak MD8h ozone concentrations (ppb) during the summer period in the (a) BASE scenario, (b) CARB scenario, (c) TECH scenario, (d) CLIM scenario, (e) FUTR-CARB scenario, and (f) FUTR+ scenario. The plot for MET scenario can be found in fig. S11.

$PM_{2.5}$ persist throughout the night.

3.1. Impact of emission control

Implementing anthropogenic emission controls using present day (2012) meteorology in the CARB and TECH scenarios significantly reduces summertime ozone concentrations throughout the state of California during the summer period (Fig. 1). The peak ozone concentration is reduced from 179 ppb in the Base scenario to 141 ppb under CARB control, and additional mitigation measures implemented in the TECH scenario further lower the peak ozone concentration to 136 ppb. In addition to the reductions in peak ozone concentrations, controlling anthropogenic emissions in the CARB and TECH scenarios nearly eliminates MD8h ozone exceedances outside of the SoCAB (Fig. 4). Although both CARB and TECH mitigation are unable to fully eliminate exceedances in the SoCAB, the sub-region experiencing the highest concentrations has been largely reduced to the northern part of the SoCAB, where population density is relatively lower (see Fig. S2). Further temporal analysis (see Fig. 3e, f) shows consistently lower MD8h ozone throughout the simulation period for both SJV and SoCAB, with higher absolute reduction in the SoCAB. The change in diurnal profile shows a different pattern in ozone reduction between SJV and SoCAB, as most of the ozone reduction happens during the day in SoCAB, while more consistent reduction happens throughout the 24-h period in SJV. Comparison of the BASE, CARB, and TECH scenarios indicates that significant reductions in ozone concentrations can be achieved by implementing anthropogenic emissions controls.

For winter $PM_{2.5}$, Fig. 2 shows that reducing anthropogenic emissions in the CARB and TECH scenarios significantly reduces the peak 24-h $PM_{2.5}$ concentration throughout the entire state. The CARB control reduces the peak $PM_{2.5}$ concentration from 74.9 $\mu g/m^3$ to 59.3 $\mu g/m^3$ while the additional mitigation measures implemented in the TECH scenario can further lower peak $PM_{2.5}$ concentrations to 53.9 $\mu g/m^3$. These reductions are due mostly to decreases in ammonium nitrate resulting from reduced NO_X and ammonia (NH_3) emissions (see Fig. S15). $PM_{2.5}$ concentration reductions result in significantly fewer exceedance episodes. As shown in Fig. 6, exceedances are reduced from 11 days to 4 days under CARB control within the SJV. Additionally, the locations of predicted exceedances are also reduced. Both the number and location of exceedances are further reduced with the additional mitigation projected in the TECH scenario. Comparatively, the mitigation of anthropogenic emissions is found to be more effective in reducing $PM_{2.5}$ exceedances in the SJV than in the SoCAB and SFBA. The temporal analysis also supports this conclusion as much higher concentration reductions can be found in Fig. 5f than Fig. 5e. Similar to ozone, the change in diurnal profiles reveals difference reduction patterns between SJV and SoCAB. In SoCAB, the diurnal profiles become flatter than the BASE scenario under emission control, as both the morning and evening peak hour concentrations are reduced. During the afternoon hours, the $PM_{2.5}$ concentration even increased slightly in the CARB scenario between 12:00–15:00 (see Fig. 5g) compared to the BASE scenario. However, the $PM_{2.5}$ concentration reduction is much more consistent throughout 24-h period in the SJV (see Fig. 5h) for CARB and TECH scenarios.

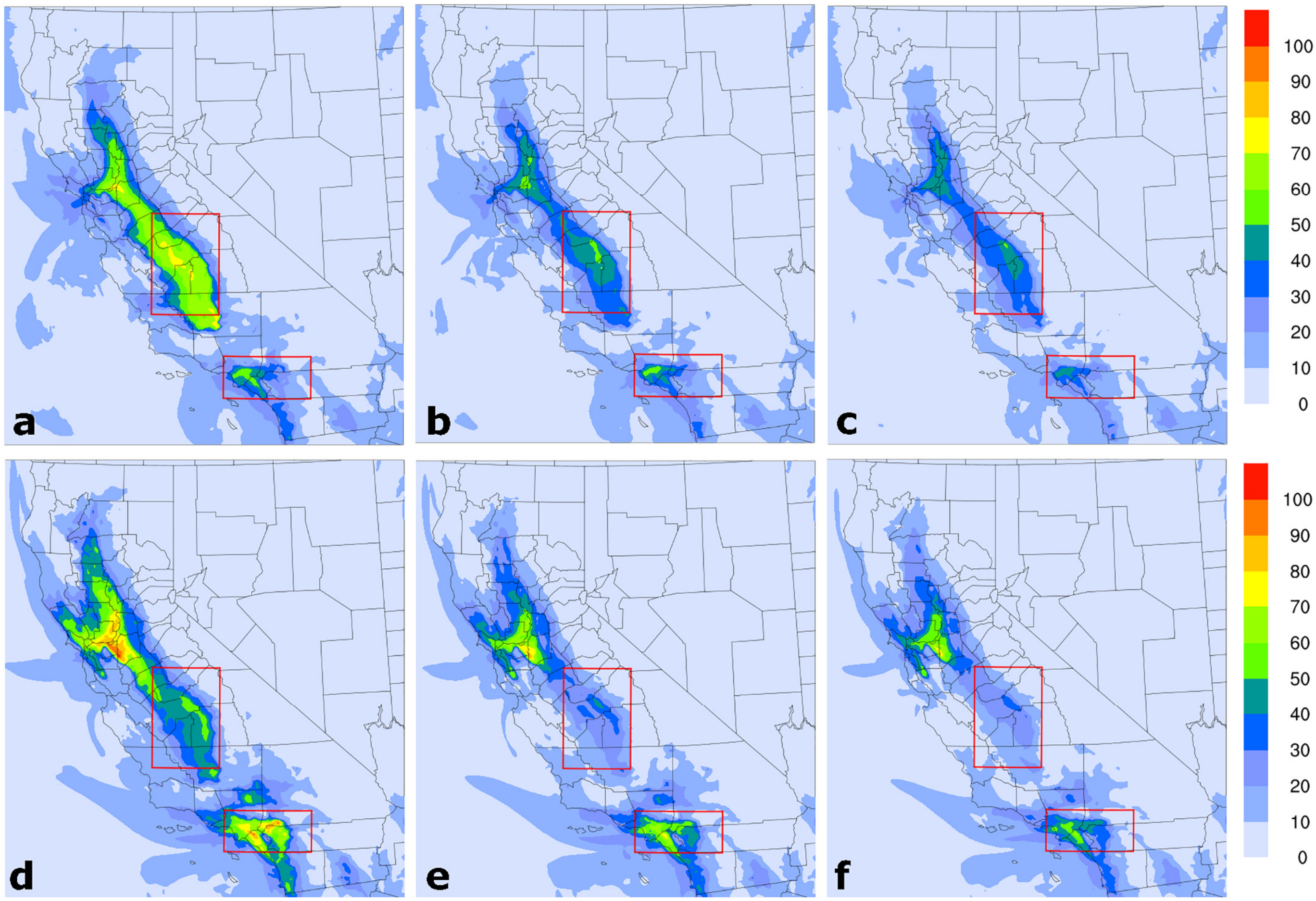

Fig. 2. Peak 24-h average $PM_{2.5}$ concentrations (μg/m^3) during the winter period in the (a) BASE scenario, (b) CARB scenario, (c) TECH scenario, (d) CLIM scenario, (e) FUTR-CARB scenario, and (f) FUTR+ scenario. The plot for MET scenario can be found in fig. S12.

3.2. Impact of climate change

During the summer period, climate change is projected to increase peak MD8h ozone concentrations from 179 ppb in the BASE scenario to 192 ppb in the MET scenario and 215 ppb in the CLIM scenario (Fig. 1 & Fig. S11). Similarly, the number of days that exceed the MD8h ozone standard increases in areas that already experienced frequent exceedances in the BASE scenario (Fig. 4 & Fig. S13). Comparison of the BASE, MET, and CLIM scenarios indicates that increases in ozone concentrations in the urban regions (SoCAB and SFBA) and rural regions (SJV) exhibit a different sensitivity to climate-driven changes in meteorological conditions and emissions. In the SJV, increases in ozone result primarily from projected changes in future meteorology (MET scenario), with climate-driven changes in emissions having little additional impact (CLIM scenario) (see Fig. 3h). Conversely, ozone concentrations in the SoCAB and SFAB increase largely in response to climate-driven increases in emissions (see Fig. 3g), mostly due to increases in biogenic emissions. Temporal analysis shows two different patterns between MET and CLIM and the BASE scenario (Fig. 3e & Fig. 3f), indicating meteorological condition are a major contributor to temporal variations. Moreover, a temperature correlation can be found between Fig. 3e & Fig. 3f and Fig. 3a & Fig. 3b, as hotter periods tends to have higher MD8h ozone concentrations (e.g., July 26–27 and Aug 22–26). Higher temperatures accelerate photochemical reaction rates, increasing the formation of ozone in these polluted regions. Similar to the CARB and TECH scenarios, the diurnal profile indicates that most of the changes happen during the daytime in SoCAB, while a consistent level of increase is observed throughout the day in SJV.

During the winter period, the changes in both biogenic and anthropogenic emissions due to climate change are very small. Therefore, results for winter $PM_{2.5}$ are nearly identical between the MET and CLIM scenarios (Fig. 2d & Fig. S12), and the difference are not observable in temporal changes (Fig. 5). However, climate-driven changes in meteorological conditions still cause significant spatial (Fig. 2) and temporal (Fig. 5) changes in wintertime $PM_{2.5}$ concentrations compared with base case levels. Compared with present-day levels, climate change is projected to increase peak wintertime $PM_{2.5}$ concentrations in the SoCAB and east SFBA, but decrease peak $PM_{2.5}$ concentrations in the SJV. Similarly, the number of days that exceed $PM_{2.5}$ NAAQS increases in the SoCAB and SFBA but decreases in the SJV (Fig. 6). Fig. 5 shows that daily variations in $PM_{2.5}$ concentrations follow a distinctly different pattern than in the BASE scenario, highlighting the influence in meteorological conditions on both gas- and particle-phase pollutants. Interestingly, changes in anthropogenic emissions appear to have a larger impact on the shape of the average diurnal profile of winter $PM_{2.5}$ than climate change, particularly in the SoCAB. Therefore, without anthropogenic emissions controls, climate change is likely to increase both the frequency and severity of pollution periods in highly populated regions (e.g., the SoCAB and SFBA) and escalate the risk for public health, consistent with previous studies (Jacob and Winner, 2009; Fiore et al., 2012; Fiore et al., 2015; Von Schneidemesser et al., 2015).

3.3. Comprehensive assessment

The previous two sections show that the two major drivers (e.g.,

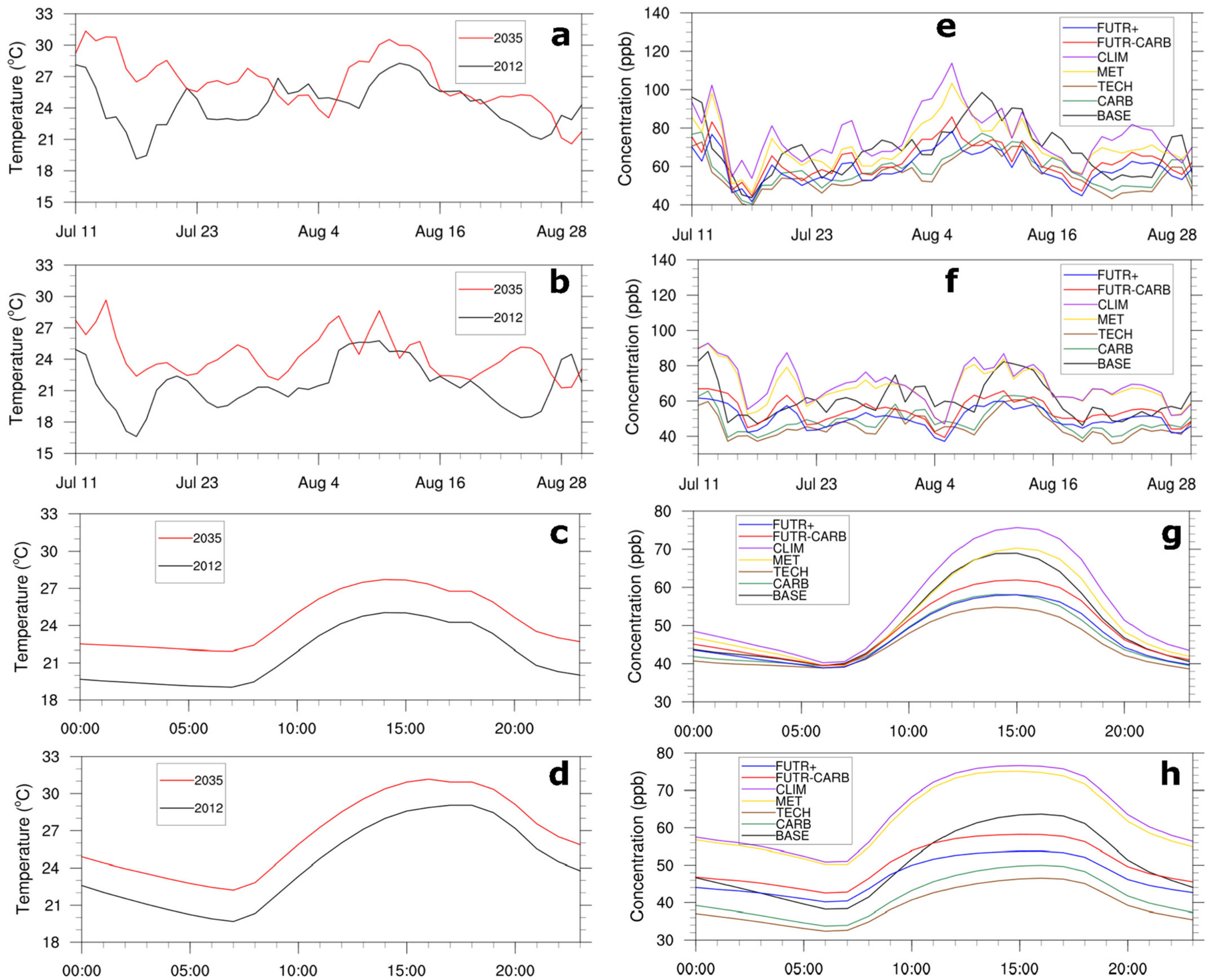

Fig. 3. Daily averaged temperature in the (a) SoCAB and (b) SJV and MD8h ozone concentrations in the (e) SoCAB and (f) SJV for each day in the summer period. Diurnal temperature profile in the (c) SoCAB and (d) SJV and diurnal ozone profile in the (g) SoCAB and (h) SJV. Diurnal profiles computed by averaging temperatures or concentrations for each hour across all days in the summer period.

climate change and emission control) generally impact future air quality in opposite directions (except for winter $PM_{2.5}$ in SJV). This section will perform a comprehensive assessment of the combined effects of both climate change and anthropogenic emission controls through FUTR-CARB and FUTR+ scenarios.

First, for summer ozone, the CARB control implemented in the FUTR-CARB scenario offsets most of the adverse impacts caused by climate change in the SoCAB and SJV. Comparing to the CLIM and BASE scenarios (Fig. 1), the FUTR-CARB scenario results in dramatic peak MD8h concentration reductions from 215 ppb in the CLIM and 179 ppb in the BASE to 158 ppb in the FUTR-CARB scenario. However, ozone concentrations in the SFBA remains higher in FUTR-CARB scenario than in the BASE scenario. Only when additional emission mitigations are applied in the FUTR+ scenario (Fig. 1f) are the climate impacts on ozone concentration fully offset in the SFBA region. The peak ozone concentration drops to 142 ppb in FUTR+, which is about the same level as CARB scenario when no climate change is considered. This result indicates that the anthropogenic emission control assumed in the TECH and FUTR+ scenario is effective in offsetting the impact of climate change, considering the reduction of peak MD8h ozone concentration is only 5 ppb between CARB and TECH but 16 ppb between FUTR-CARB and FUTR+. Although the FUTR+ scenario achieves almost the same peak MD8h ozone concentration as CARB scenario, the area and frequency of nonattainment exceedance in FUTR+ is still larger than CARB scenario (Fig. 4f & Fig. 4b), especially for SFBA regions, as a result of the climate change penalty. Additional analysis on temporal variation shows that meteorological conditions still dominate the overall trends in ozone concentrations as observed in MET and CLIM scenarios (Fig. 5e & Fig. 5f). Furthermore, the diurnal profiles (Fig. 5g & Fig. 5h) indicate that the FUTR+ scenario achieved a similar level of ozone concentrations as the CARB scenario in the SoCAB region, but not in the SJV. In the SJV, the average ozone concentration is still about 4 ppb higher in the FUTR+ scenario than in the CARB scenario. Nevertheless, the effectiveness of emissions mitigation in offsetting climate change penalty on ozone pollution is demonstrated through the comparison between FUTR+ and CARB results.

For winter $PM_{2.5}$, both emission mitigation and climate change reduce peak $PM_{2.5}$ concentrations within the SJV in the FUTR-CARB scenario relative to the TECH scenario (Fig. 2e & Fig. 2b). In the FUTR + scenario, peak levels are lower than 30 $\mu g/m^3$ throughout most of the SJV (Fig. 2f), almost eliminating NAAQS exceedances in the SJV (Fig. 6f). However, for urban regions such as SFBA and SoCAB, both

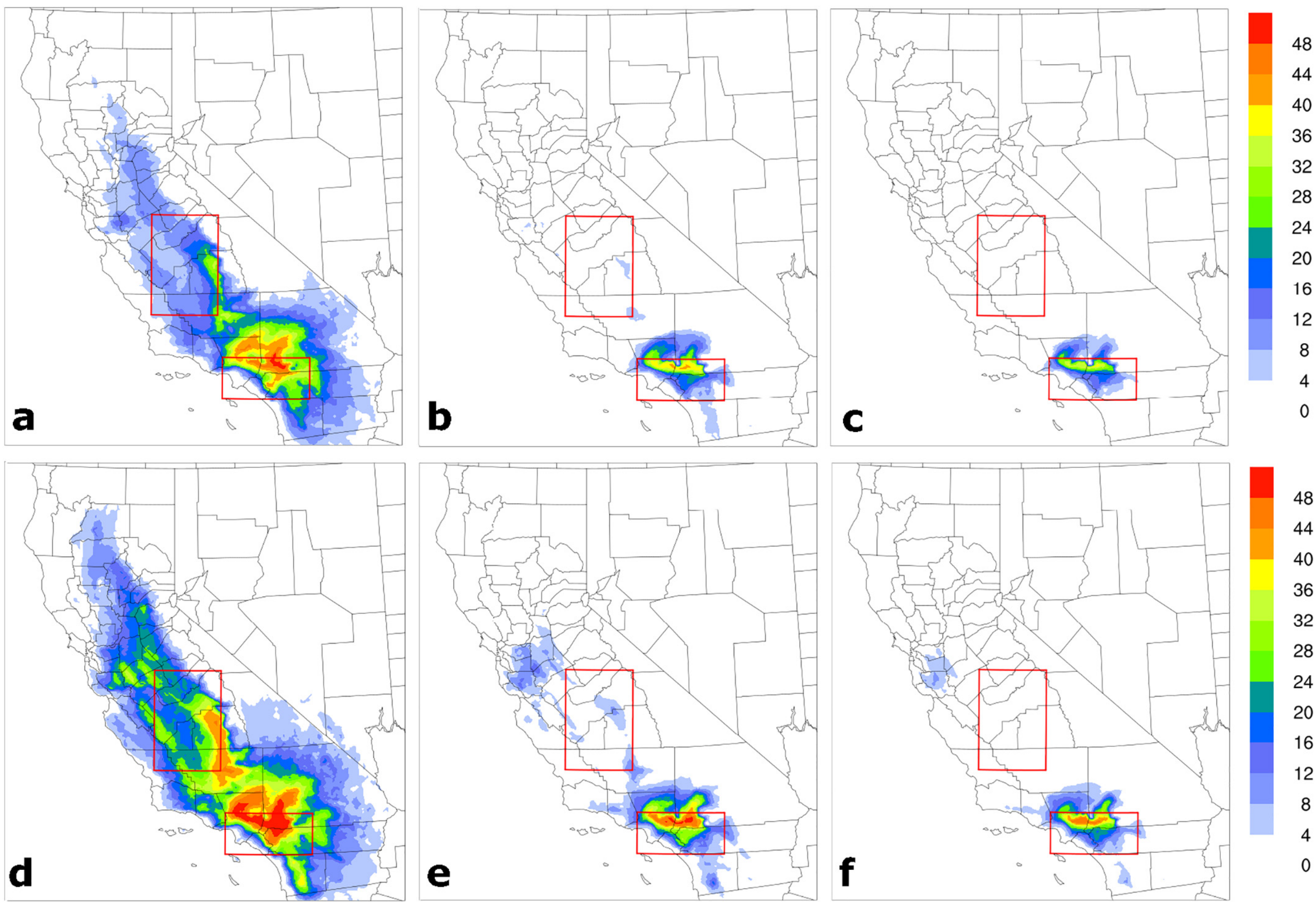

Fig. 4. The number of days the 70 ppb MD8h ozone standard is exceeded during the summer period in the (a) BASE scenario, (b) CARB scenario, (c) TECH scenario, (d) CLIM scenario, (e) FUTR-CARB scenario, (f) FUTR+ scenario out of a total of 51 simulation days. The plot for MET scenario can be found in fig. S13.

emission mitigation strategies are insufficient to fully offset the climate change penalty to $PM_{2.5}$ concentrations. In the FUTR-CARB and FUTR + scenarios, the peak $PM_{2.5}$ concentrations are increased in SoCAB from the BASE and CARB scenarios (Fig. 2). For the eastern SFBA, the peak $PM_{2.5}$ concentrations remain at levels similar to the BASE scenario, while peak $PM_{2.5}$ concentrations are increased in populated areas including San Jose. Additionally, the composition of future $PM_{2.5}$ in SFBA and SoCAB regions is likely to change, with increases in organic constituents and decreases in inorganic components (see Fig. S15). Impacts are also reflected in the number of exceedances (Fig. 6), with exceedances predicted to occur in higher frequencies and over larger areas in the SoCAB and SFBA in both the FUTR-CARB & FUTR+ scenarios relative to the BASE case. As observed with summer ozone, the temporal profiles show similar patterns between CLIM and FUTR-CARB and FUTR+ scenarios relative to the BASE scenario due to the different meteorological conditions (see Fig. 5). Although the FUTR+ scenario has lower $PM_{2.5}$ concentration than the FUTR-CARB scenario, the difference is much larger during high concentration days in both the SoCAB and the SJV. The diurnal profiles (Fig. 5h) show the lowest and least dynamic pattern in the FUTR+ scenario in the SJV. For the SoCAB region the diurnal profiles (Fig. 5g) indicate a higher $PM_{2.5}$ concentration during daytime in the FUTR+ scenario when compared to the BASE scenario, while concentrations are constantly higher in the FUTR-CARB scenario than the BASE scenario. Additional details regarding the temporal analysis can be found in Section 2 of the SI.

3.4. Health and social economic benefit

The results of the health impact assessment demonstrate a large net cost (i.e., increases in detrimental health effects) from air quality impacts due to climate change: approximately 35 million \$/day due to increased winter $PM_{2.5}$ and > 54 million \$/day due to increased summer O_3 (see results for CLIM case in Fig. 7). Under current meteorological conditions the implementation of CARB control measures achieves significant economic benefits of approximately 26 and 27 million \$/day for winter $PM_{2.5}$ and summer O_3, respectively. The benefits of CARB emission controls can offset the impacts of climate change on winter $PM_{2.5}$, providing a net benefit of 4.35 million \$/day. However, improvements are not enough to offset the impacts of climate change on summer O_3, as the FUTR-CARB scenario attains a net cost of around 13 million \$/day. Only in the FUTR+ scenario, which includes expansion of emissions mitigation strategies beyond those in the CARB scenario are the impacts of climate change fully compensated for regarding summer O_3, with a net benefit of almost 10 million \$/day. More details about the health and social economic benefits for different endpoints (including myocardial infarction, asthma, respiratory symptoms, and others) can be found in Table S5 and Table S6.

Fig. S16 shows the spatial distribution of the health benefits valuation for the CLIM, FUTR-CARB, and FUTR+ scenarios. For summer O_3, the impact of climate change leads to a net health cost throughout almost the entire state. Some areas revert to net health benefits under CARB control, and expanded areas transition to net benefits in the TECH scenario. However, two of the main population centers (SFBA and SoCAB) continue to experience net health cost. For winter $PM_{2.5}$,

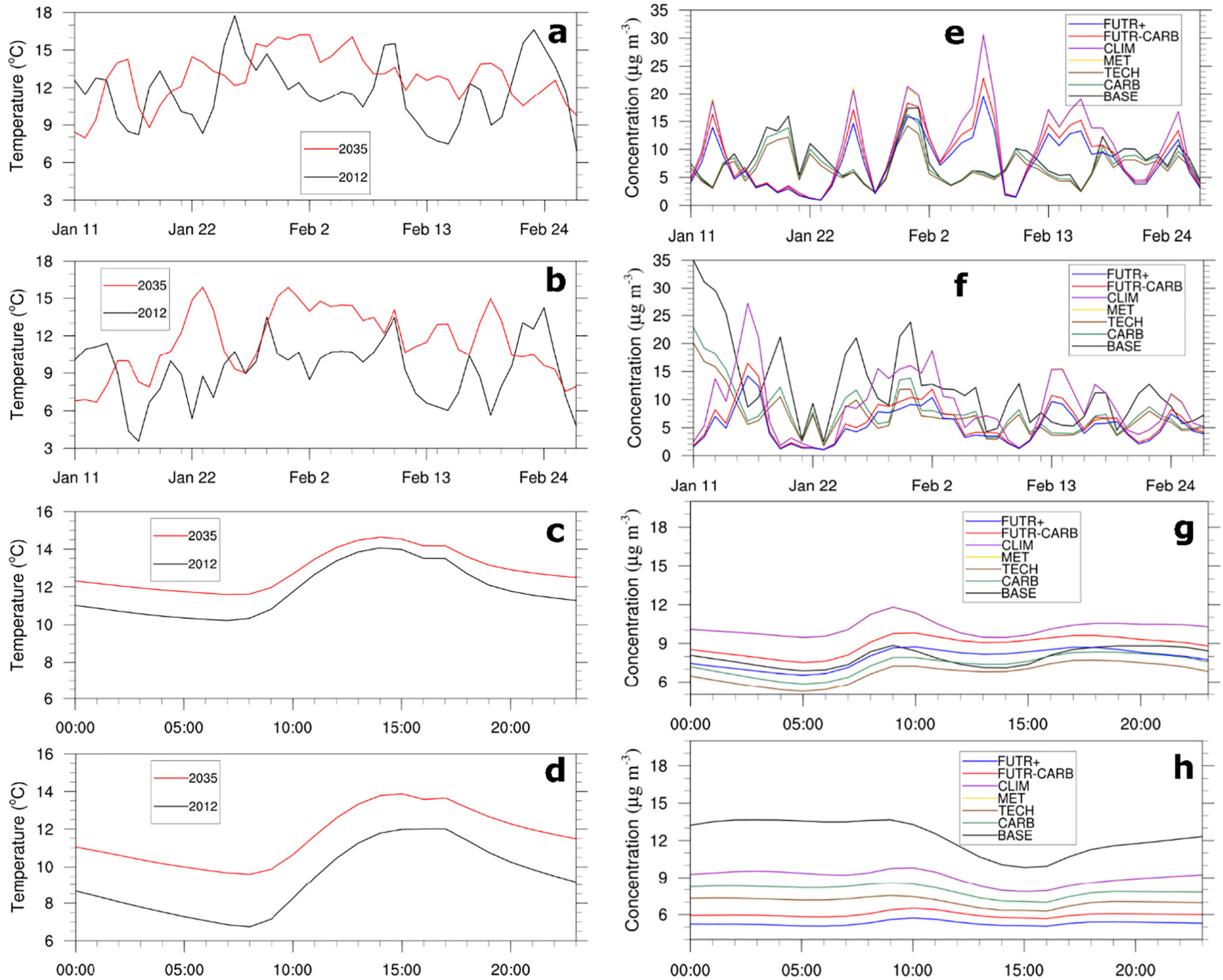

Fig. 5. Daily averaged temperature in the (a) SoCAB and (b) SJV and 24-h average $PM_{2.5}$ concentrations in the (e) SoCAB and (f) SJV for each day in the winter period. Diurnal temperature profile in the (c) SoCAB and (d) SJV and diurnal $PM_{2.5}$ profile in the (g) SoCAB and (h) SJV. Diurnal profiles computed by averaging temperatures or concentrations for each hour across all days in the winter period.

the impacts of climate change are also associated with large negative health impacts that generally correspond to population centers. While the CARB control shows health improvements for the SJV region, most of the SFBA and the coastal part of SoCAB and San Diego experience net negative health effects. In the FUTR+ scenario, positive health improvements are achieved in the most populated regions of SFBA & SoCAB, including most of Los Angeles, San Francisco and San Jose. However, some of the suburban areas of SoCAB and north SFBA still experience net health costs, although the cost is reduced compared to the FUTR-CARB scenario in most of these areas. Additionally, a few less populated areas of SoCAB experience a reversal of net benefit in the FUTR-CARB scenario to net cost in the FUTR+ scenario, demonstrating the complexity and uncertainty of emission mitigation outcomes.

4. Conclusions

In this study we analyze the impact of major drivers of future air quality in California, both separately and simultaneously, for the year 2035. A variety of different scenarios are considered (Table 1) to quantify and compare the potential air quality impacts of future changes in climate and emissions and provide a comprehensive assessment of near-term future air quality in California. Both spatial and temporal trends in air pollutant concentrations are examined in detail, using the metrics described in Section 2. Results for the MET scenario indicates that climate-driven changes in meteorological conditions will significantly alter day-to-day variations in future ozone and $PM_{2.5}$ concentrations, likely increasing the frequency and severity of pollution periods in highly populated areas and escalating the risk for public health. Increases in biogenic and anthropogenic emissions due to climate change are important during the summer season in some areas but have little effect on pollutant concentrations during the winter. Reductions in anthropogenic emissions in the CARB scenario tend to decrease ozone and $PM_{2.5}$ concentrations on days when concentrations are highest, and further reduction in $PM_{2.5}$ and O_3 concentrations are found with a more aggressive emission control strategy in the TECH scenario. Overall, the adoption of alternative energy technologies and strategies in pursuit of GHG reductions can achieve reductions in atmospheric pollution above and beyond those achieved in current regulatory planning, which becomes increasingly important in offsetting the impacts of climate change. The two main drivers of future air quality are found to be climate change and reductions in anthropogenic emissions.

Results indicate that climate change may cause negative impacts on air quality at a large scale in California, leading to significant social economic costs resulting from adverse health effects. Indeed, the impact

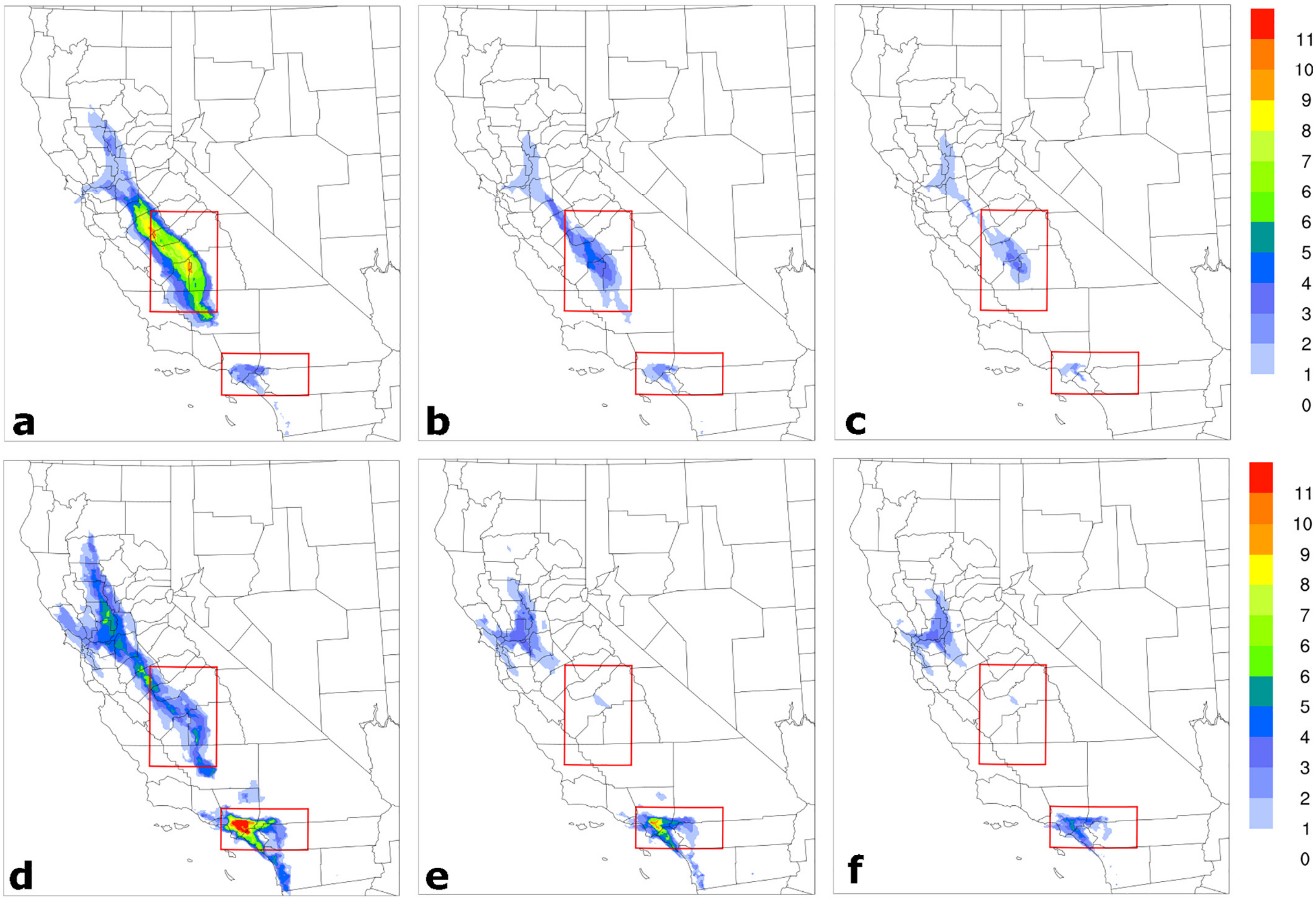

Fig. 6. The number of days the 24-h average 35 μg/m^3 $PM_{2.5}$ air quality standard is exceeded during the winter period in the (a) BASE scenario, (b) CARB scenario, (c) TECH scenario, (d) CLIM scenario, (e) FUTR-CARB scenario, (f) FUTR + scenario out of a total of 47 simulation days. The plot for MET scenario can be found in fig. S14.

of climate change may result in current emission mitigation planning strategies failing to achieve targeted outcomes including compliance with regulatory standards and avoidance of societal and economic costs from human exposure. This outcome is more pronounced for the summer ozone period, indicating that strategies to reduce ozone precursor emissions including NO_x and VOC may need to be considered seasonally, i.e., greater reductions targeted during summer periods. However, the implementation of aggressive alternative energy strategies in pursuit of GHG reductions can offset the impacts of climate change for both winter and summer, demonstrating a path forward to achieving air quality and human health benefits. The benefits of additional emission reduction measures are most effective in rural and suburban areas, with urban population centers continuing to experience degraded health effects under climate change impacted air quality. Therefore, populated regions may require more stringent control than is currently anticipated. Additionally, potentially effective adaptation measures may include the migration of population sub-sets with heightened vulnerability to air quality induced disease from urban to rural areas.

Although this study focused on California, many of the results

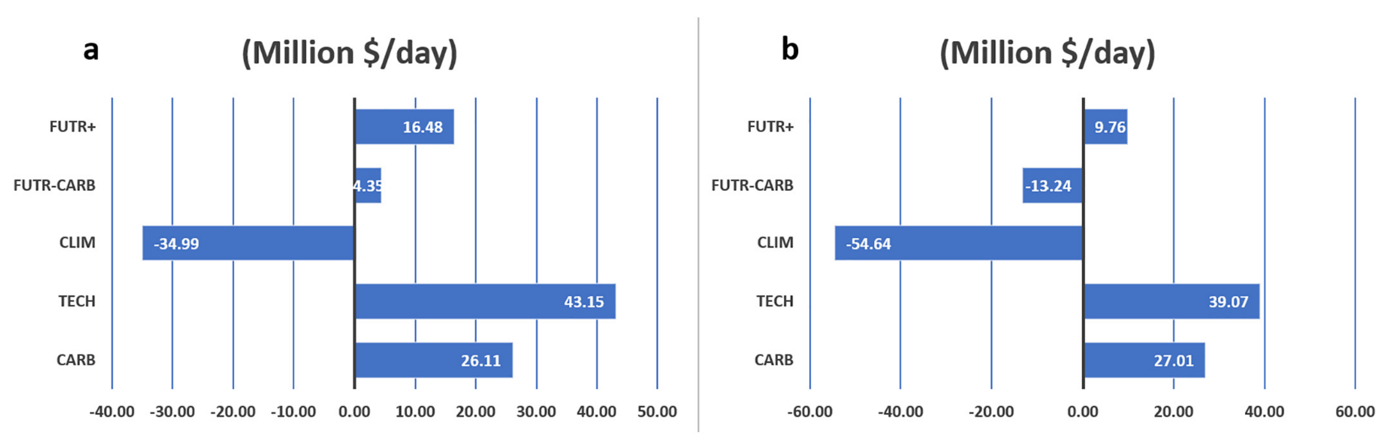

Fig. 7. The economic valuation of health impact under different scenarios compared to the BASE scenario for (a) winter $PM_{2.5}$ and (b) summer O_3.

presented here have general implication for extrapolation to other regions, especially those with highly populated urban areas and pre-existing degraded air quality conditions. Generally, mitigation planning for regions experiencing poor air quality (e.g., China) should consider climate change impacts in the design of emission reduction strategies. In particular, the use of renewable energy in tandem with efficiency measures and end-use electrification to significantly reduce emissions and offset climate change impacts can be an effective strategy in many world regions. However, differences in renewable resource availability and other factors will require unique consideration of energy system design and deployment across regions. For example, California has considerable wind and solar power resources which have enabled high renewable penetrations in response to policy mandates, and the bulk of the remaining in-state generation is provided from natural gas power plants. Thus, the California electricity mix is reasonably clean relative to other regions and enables significant environmental benefits from end-use electrification. However, in regions lacking high levels of wind and solar availability, additional renewable resources (e.g., geothermal, wave, tidal, hydropower) or other low carbon power generation strategies including nuclear power may need to be considered to attain the same GHG and AQ benefits. Furthermore, in regions with higher emitting fossil fuel plants, e.g., those with significant amounts of coal generation, electrification may not attain emission reductions with the same effectiveness as it does in regions with high renewable or lower emitting technology mixes. Therefore, emission mitigation planning should carefully consider regional energy systems in the development of strategies to offset the impacts of climate change.

Acknowledgements

This publication was developed under Assistance Agreement No. EPA 83588101 awarded by the U.S. Environmental Protection Agency to the Regents of the University of California. It has not been formally reviewed by EPA. The views expressed in this document are solely those of the authors and do not necessarily reflect those of the Agency. EPA does not endorse any products or commercial services mentioned in this publication. The authors would like to gratefully acknowledge the assistance from the UCI High Performance Computing group and the UCI Research Computing group, and funding support from the UCI Advanced Power and Energy Program. The authors would like to acknowledge the contribution of Energy and Environmental Economics to the development of the future energy technology scenario, with a specific thanks to Zachary Subin. Additionally, the authors wish to thank Victor Vila and Pau Balatga for their important scientific contributions, and thank Gang Chen for proof read.

Appendix A. Supplementary data

Supplementary data to this article can be found online at https://doi.org/10.1016/j.envint.2019.02.007.

References

Aw, J., Kleeman, M.J., 2003. Evaluating the first-order effect of intraannual temperature variability on urban air pollution. J. Geophys. Res. 108 (D12), 4365. https://doi.org/10.1029/2002JD002688.

Benosa, G., et al., 2018. Air quality impacts of implementing emission reduction strategies at southern California airports. Atmos. Environ. 185, 121–127. https://doi.org/10.1016/j.atmosenv.2018.04.048.

Brasseur, G.P., et al., 2006. Impact of climate change on the future chemical composition of the global troposphere. J. Clim. 19 (16), 3932–3951. https://doi.org/10.1175/JCLI3832.1.

California Air Resources Board, 2016. CEPAM: 2016 SIP - standard emissions tool. https://www.arb.ca.gov/app/emsinv/fcemssumcat/fcemssumcat2016.php, Accessed date: June 2018.

California DOF, 2017. Population projections (Baseline 2016). State of California. Sacramento, CA: Department of Finance. Available at: http://www.dof.ca.gov/Forecasting/Demographics/projections/.

Campbell, P., et al., 2018. Impacts of transportation sector emissions on future U.S. air quality in a changing climate. Part II: air quality projections and the interplay between emissions and climate change. Environ. Pollut. 238, 918–930. https://doi.org/10.1016/j.envpol.2018.03.016.

CARB, 2005. Characterization of ambient PM10 and PM2.5 in California. Available at: https://www.arb.ca.gov/pm/pmmeasures/pmch05/stateover05.pdf.

CARB, 2013. Current CARB emissions inventory (ver. 2012). Available at: https://www.arb.ca.gov/ei/emsinv2012.php, Accessed date: 11 October 2017.

CARB, 2017a. Area Designation Maps/State and National. California Air Resources Board. Available at: https://www.arb.ca.gov/desig/adm/adm.htm, Accessed date: 6 April 2018.

CARB, 2017b. CEPAM: 2016 SIP - standard emission tool emission projections by summary category base year: 2012, California Air Resources Board. https://www.arb.ca.gov/app/emsinv/fcemssumcat/fcemssumcat2016.php, Accessed date: June 2018.

Carreras-Sospedra, M., et al., 2006. Air quality modeling in the south coast air basin of California: what do the numbers really mean? J. Air Waste Manage. Assoc. 56 (8), 1184–1195. https://doi.org/10.1080/10473289.2006.10464530.

Carter, W.P.L., 2010. Development of the SAPRC-07 chemical mechanism. Atmos. Environ. 44 (40), 5324–5335. https://doi.org/10.1016/j.atmosenv.2010.01.026.

Collet, S., et al., 2014. Evaluation of light-duty vehicle mobile source regulations on ozone concentration trends in 2018 and 2030 in the western and eastern United States. J. Air Waste Manage. Assoc. 64 (2), 175–183.

Davidson, K., et al., 2007. Analysis of PM2. 5 using the environmental benefits mapping and analysis program (BenMAP). J. Toxic. Environ. Health A 70 (3–4), 332–346.

Ebi, K.L., McGregor, G., 2008. Climate change, tropospheric ozone and particulate matter, and health impacts. Environ. Health Perspect. 116 (11), 1449–1455. https://doi.org/10.1289/ehp.11463.

Ebrahimi, S., Mac Kinnon, M., Brouwer, J., 2018. California end-use electrification impacts on carbon neutrality and clean air. Appl. Energy 213, 435–449. https://doi.org/10.1016/j.apenergy.2018.01.050.

Emery, C., et al., 2017. Recommendations on statistics and benchmarks to assess photochemical model performance. J. Air Waste Manage. Assoc. 67 (5), 582–598. https://doi.org/10.1080/10962247.2016.1265027.

Emmons, L.K., Walters, S., Hess, P.G., Lamarque, J.-F., Pfister, G.G., Fillmore, D., Granier, C., Guenther, A., Kinnison, D., Laepple, T., Orlando, J., Tie, X., Tyndall, G., Wiedinmyer, C., Baughcum, S.L., Kloster, S., 2010. Description and evaluation of the Model for Ozone and Related chemical Tracers, version 4 (MOZART-4). Geosci. Model Dev. 3, 43–67. https://doi.org/10.5194/gmd-3-43-2010.

EPA, 2018. Current nonattainment counties for all criteria pollutants, United States Environmental Protection Agency. Available at: https://www3.epa.gov/airquality/greenbook/ancl.html, Accessed date: 25 March 2018.

Erickson, E., Jennings, M., 2017. Energy, transportation, air quality, climate change, health Nexus: sustainable energy is good for our health. AIMS Publ. Health 4 (1), 47–61. https://doi.org/10.3934/publichealth.2017.1.47.

Fann, N., et al., 2015. The geographic distribution and economic value of climate change-related ozone health impacts in the United States in 2030. J. Air Waste Manage. Assoc. 65 (5), 570–580. https://doi.org/10.1080/10962247.2014.996270.

Fiore, A.M., et al., 2012. Global air quality and climate. Chem. Soc. Rev. 41 (19), 6663. https://doi.org/10.1039/c2cs35095e.

Fiore, A.M., Naik, V., Leibensperger, E.M., 2015. Air quality and climate connections. J. Air Waste Manage. Assoc. 65 (6), 645–685. https://doi.org/10.1080/10962247.2015.1040526.

Franco, G., Sanstad, A.H., 2008. Climate change and electricity demand in California. Clim. Chang. 87 (S1), 139–151. https://doi.org/10.1007/s10584-007-9364-y.

Friedl, M.A., et al., 2010. MODIS collection 5 global land cover: algorithm refinements and characterization of new datasets. Remote Sens. Environ. 114 (1), 168–182. https://doi.org/10.1016/j.rse.2009.08.016.

Fuzzi, S., et al., 2015. Particulate matter, air quality and climate: lessons learned and future needs. Atmos. Chem. Phys. 15 (14), 8217–8299. https://doi.org/10.5194/acp-15-8217-2015.

Gao, Y., et al., 2013. The impact of emission and climate change on ozone in the United States under representative concentration pathways (RCPs). Atmos. Chem. Phys. 13 (18), 9607–9621. https://doi.org/10.5194/acp-13-9607-2013.

Giorgetta, M.A., et al., 2013. Climate and carbon cycle changes from 1850 to 2100 in MPI-ESM simulations for the coupled model Intercomparison project phase 5. J. Adv. Model. Earth Syst. 5 (3), 572–597. https://doi.org/10.1002/jame.20038.

Guenther, A., et al., 2006. Estimates of global terrestrial isoprene emissions using MEGAN (model of emissions of gases and aerosols from nature). Atmos. Chem. Phys. 6 (11), 3181–3210. https://doi.org/10.5194/acpd-6-107-2006.

Hart, E.K., Jacobson, M.Z., 2012. The carbon abatement potential of high penetration intermittent renewables. Energy Environ. Sci. 5 (5), 6592. https://doi.org/10.1039/c2ee03490e.

He, H., et al., 2016. Future U.S. ozone projections dependence on regional emissions, climate change, long-range transport and differences in modeling design. Atmos. Environ. 128, 124–133. https://doi.org/10.1016/j.atmosenv.2015.12.064.

Heald, C.L., et al., 2008. Predicted change in global secondary organic aerosol concentrations in response to future climate, emissions, and land use change. J. Geophys. Res. Atmos. 113 (D5). https://doi.org/10.1029/2007JD009092. (p. n/a-n/a).

Hong, S.-Y., Noh, Y., Dudhia, J., 2006. A new vertical diffusion package with an explicit treatment of entrainment processes. Mon. Weather Rev. 134 (9), 2318–2341.

Horne, J.R., Dabdub, D., 2017. Impact of global climate change on ozone, particulate matter, and secondary organic aerosol concentrations in California: a model perturbation analysis. Atmos. Environ. 153, 1–17. https://doi.org/10.1016/j.atmosenv.2016.12.049.

Industrial Economics, 2016a. Literature Review of Air Pollution-Related Health Endpoints and Concentration-Response Functions for Particulate Matter: Results and Recommendations. Memorandum. Industrial Economics, Inc, Cambridge, MA

Available at: http://www.aqmd.gov/docs/default-source/clean-air-plans/socioeconomic-analysis/iec_pmlitreview_092916.pdf.
Industrial Economics, 2016b. Literature Review of Air Pollution-Related Health Endpoints and Concentration-Response Functions for Ozone, Nitrogen Dioxide, and Sulfur Dioxide: Results and Recommendations. Memorandum. Industrial Economics, Inc, Cambridge, MA Available at: http://www.aqmd.gov/docs/default-source/clean-air-plans/socioeconomic-analysis/iec_gasplitreview_092916.pdf.
Industrial Economics, 2016c. Review of Baseline Incidence Rate Estimates for Use in 2016 Socioeconomic Assessment. Memorandum. Industrial Economics, Inc, Massachusetts, MA Available at: http://www.aqmd.gov/docs/default-source/clean-air-plans/socioeconomic-analysis/iecmemos_november2016/scbaselineincidence_112916.pdf.
Industrial Economics, Robinson, Lisa, 2016a. Review of Morbidity Valuation Estimates for Use in 2016 Socioeconomic Assessment. Memorandum. Industrial Economics, Inc, Massachusetts, MA Available: http://www.aqmd.gov/docs/default-source/clean-air-plans/socioeconomic-analysis/iecmemos_november2016/scmorbidityvaluation_112816.pdf.
Industrial Economics, Robinson, Lisa, 2016b. Review of Mortality Risk Reduction Valuation Estimates for 2016 Socioeconomic Assessment. Memorandum. Industrial Economics, Inc, Massachusetts, MA Available: http://www.aqmd.gov/docs/default-source/clean-air-plans/socioeconomic-analysis/iecmemos_november2016/evaluationcriteria_113016.pdf.
IPCC, 2014. In: Barros, Vicente R. (Ed.), Fifth Assessment Report (AR5): Climate Change 2013/2014: Climate Change 2014: Impacts, Adaptation, and Vulnerability; Part B. Regional Aspects. Univer. Cambridge University Press (Working Group II Co-Chair, Centro de Investigaciones Del Mar Y la Atmósfera).
Jacob, D.J., Winner, D.A., 2009. Effect of climate change on air quality. Atmos. Environ. 43 (1), 51–63. https://doi.org/10.1016/j.atmosenv.2008.09.051.
Jacobson, M.Z., Colella, W.G., Golden, D.M., 2005. Cleaning the air and improving health with hydrogen fuel-cell vehicles. Science 308 (5730), 1901–1905.
Jacobson, M.Z., et al., 2015. 100% clean and renewable wind, water, and sunlight (WWS) all-sector energy roadmaps for the 50 United States. Energy Environ. Sci. 8 (7), 2093–2117.
Kampa, M., Castanas, E., 2008. Human health effects of air pollution. Environ. Pollut. 151 (2), 362–367. https://doi.org/10.1016/j.envpol.2007.06.012.
Kelly, J., Makar, P.A., Plummer, D.A., 2012. Projections of mid-century summer air-quality for North America: effects of changes in climate and precursor emissions. Atmos. Chem. Phys. 12 (12), 5367–5390. https://doi.org/10.5194/acp-12-5367-2012.
Kinney, P.L., 2018. Interactions of climate change, air pollution, and human health. Cur. Environ. Health Rep. https://doi.org/10.1007/s40572-018-0188-x.
Kinnon, M. Mac, et al., 2019. Considering future regional air quality impacts of the transportation sector. Energy Policy 124, 63–80. https://doi.org/10.1016/j.enpol.2018.09.011.
Kleeman, M.J., 2008. A preliminary assessment of the sensitivity of air quality in California to global change. Clim. Chang. 87 (S1), 273–292. https://doi.org/10.1007/s10584-007-9351-3.
Lee, Y., et al., 2016. Potential impact of a US climate policy and air quality regulations on future air quality and climate change. Atmos. Chem. Phys. 16 (8), 5323–5342. https://doi.org/10.5194/acp-16-5323-2016.
Liao, H., Chen, W.T., Seinfeld, J.H., 2006. Role of climate change in global predictions of future tropospheric ozone and aerosols. J. Geophys. Res. Atmos. 111 (12), 1–18. https://doi.org/10.1029/2005JD006852.
Lin, G., Penner, J.E., Zhou, C., 2016. How will SOA change in the future? Geophys. Res. Lett. 43 (4), 1718–1726. https://doi.org/10.1002/2015GL067137.
Loughlin, D.H., Benjey, W.G., Nolte, C.G., 2011. ESP v1. 0: methodology for exploring emission impacts of future scenarios in the United States. Geosci. Model Dev. 4, 287–297.
Mahmud, A., et al., 2008. Statistical downscaling of climate change impacts on ozone concentrations in California. J. Geophys. Res. 113 (D21), D21103. https://doi.org/10.1029/2007JD009534.
Mahmud, A., et al., 2010. Climate impact on airborne particulate matter concentrations in California using seven year analysis periods. Atmos. Chem. Phys. 10 (22), 11097–11114. https://doi.org/10.5194/acp-10-11097-2010.
Mahmud, A., Hixson, M., Kleeman, M.J., 2012. Quantifying population exposure to airborne particulate matter during extreme events in California due to climate change. Atmos. Chem. Phys. 12 (16), 7453–7463. https://doi.org/10.5194/acp-12-7453-2012.
Mahone, A., et al., 2018. Deep Decarbonization in a High Renewables Future: Updated Results from the California PATHWAYS Model. Sacramento, CA.
Millstein, D.E., Harley, R.A., 2009. Impact of climate change on photochemical air pollution in Southern California. Atmos. Chem. Phys. 9 (2004), 3745–3754. https://doi.org/10.5194/acp-9-3745-2009.
Monaghan, A.J., et al., 2014. NCAR CESM Global Bias-Corrected CMIP5 Output to Support WRF/MPAS Research. Boulder CO: Research Data Archive at the National Center for Atmospheric Research, Computational and Information Systems Laboratoryhttps://doi.org/10.5065/D6DJ5CN4.
Morrison, G.M., et al., 2015. Comparison of low-carbon pathways for California. Clim. Chang. 131 (4), 545–557.
Motallebi, N., et al., 2008. Climate change impact on California on-road mobile source emissions. Clim. Chang. 87 (1), 293–308.
(updated daily) National Centers for Environmental Prediction/National Weather Service/NOAA/U.S. Department of Commerce, 2000. NCEP FNL Operational Model Global Tropospheric Analyses, continuing from July 1999. Research Data Archive at the National Center for Atmospheric Research, Computational and Information Systems Laboratoryhttps://doi.org/10.5065/D6M043C6 , Accessed date: 8 July 2018.
Nsanzineza, R., et al., 2017. Emissions implications of downscaled electricity generation scenarios for the western United States. Energy Policy 109, 601–608.
ORNL, 2016. LandScan. Oak Ridge National Laboratory, Oak Ridge, TN Available at: http://web.ornl.gov/sci/landscan/.
Pye, H.O.T.T., et al., 2013. Epoxide pathways improve model predictions of isoprene markers and reveal key role of acidity in aerosol formation. Environ. Sci. Technol. 47 (19), 11056–11064. https://doi.org/10.1021/es402106h.
Racherla, P.N., Adams, P.J., 2006. Sensitivity of global tropospheric ozone and fine particulate matter concentrations to climate change. J. Geophys. Res. Atmos. 111 (24), 1–11. https://doi.org/10.1029/2005JD006939.
Sacks, J.D., et al., 2018. The environmental benefits mapping and analysis program–community edition (BenMAP–CE): a tool to estimate the health and economic benefits of reducing air pollution. Environ. Model Softw. 104, 118–129.
Shen, E., Oliver, A., Dabirian, S., 2017. Final Socioeconomic Report. South Coast Air Quality Management District Available at: http://www.aqmd.gov/docs/default-source/clean-air-plans/socioeconomic-analysis/final/sociofinal_030817.pdf?sfvrsn=2.
Steiner, A.L., et al., 2006. Influence of future climate and emissions on regional air quality in California. J. Geophys. Res. Atmos. 111 (18), 1–22. https://doi.org/10.1029/2005JD006935.
Tai, A.P.K., Mickley, L.J., Jacob, D.J., 2010. Correlations between fine particulate matter (PM2.5) and meteorological variables in the United States: implications for the sensitivity of PM2.5 to climate change. Atmos. Environ. 44 (32), 3976–3984. https://doi.org/10.1016/j.atmosenv.2010.06.060.
U.S. EPA, 2018. Nonattainment Areas for Criteria Pollutants (Green Book). Available at: https://www.epa.gov/green-book, Accessed date: 8 March 2018.
Val Martin, M., et al., 2015. How emissions, climate, and land use change will impact mid-century air quality over the United States: a focus on effects at national parks. Atmos. Chem. Phys. 15 (5), 2805–2823. https://doi.org/10.5194/acp-15-2805-2015.
Von Schneidemesser, E., et al., 2015. Chemistry and the linkages between air quality and climate change. Chem. Rev. 115 (10), 3856–3897. https://doi.org/10.1021/acs.chemrev.5b00089.
Williams, J.H., et al., 2012. The technology path to deep greenhouse gas emissions cuts by 2050: the pivotal role of electricity. Science 335 (6064), 53–59.
Zapata, C.B., et al., 2018. Low-carbon energy generates public health savings in California. Atmos. Chem. Phys. 18 (7), 4817–4830. https://doi.org/10.5194/acp-18-4817-2018.
Zhang, Y., et al., 2017. Co-benefits of global, domestic, and sectoral greenhouse gas mitigation for US air quality and human health in 2050. Environ. Res. Lett. 12 (11), 114033.